Supplementary Material (ESI) for Journal of Materials Chemistry

Supporting Information

Soft Shape Memory in Main-Chain Liquid Crystalline Elastomers

Kelly A. Burke[1,2] and Patrick T. Mather[2,3*]

[1]Department of Macromolecular Science and Engineering, Case Western Reserve University, 2100 Adelbert Road, Cleveland, OH 44106, USA

[2]Syracuse Biomaterials Institute, [3]Department of Biomedical and Chemical Engineering, Syracuse University, 121 Link Hall, Syracuse, NY 13244, USA

*ptmather@syr.edu

Wide-angle x-ray scattering. The wide-angle x-ray scattering patterns for stretched ***5H-5tB*** LCEs were studied to assist in identifying the smectic phase. To prepare samples, slender rectangular films (typical dimensions: 5 mm x 1 mm x 0.4 mm) were mounted in the DMA under slight tensile load (5-6 kPa). A shape memory experiment using a maximum stress of 100 kPa was run on the sample as described in the manuscript, except instead of heating to T_{upper} during the final step to fully recover the sample, the sample was heated to 25 °C and held for 45 minutes before unloading. The samples fixed strain well, and an extended isothermal annealing step was employed to minimize relaxation during the x-ray exposure. Shown below in Fig. S1 are eight WAXS patterns for the four ***5H-5tB*** LCEs studied in this paper. Two exposures were collected for each sample to allow study of the smectic layer reflections, shown as a four point pattern in the top row images collected at a sample to detector distance of 236.4 mm, the siloxane reflections, shown in both the top and bottom row images as a ring with relatively little anisotropy, and the mesogen reflections, shown as split equatorial reflections in the bottom row images collected at a sample to detector distance of 65.7 mm. In all cases, the patterns of these oriented samples are consistent with a chevron-type architecture observed in smectic-C LCEs.

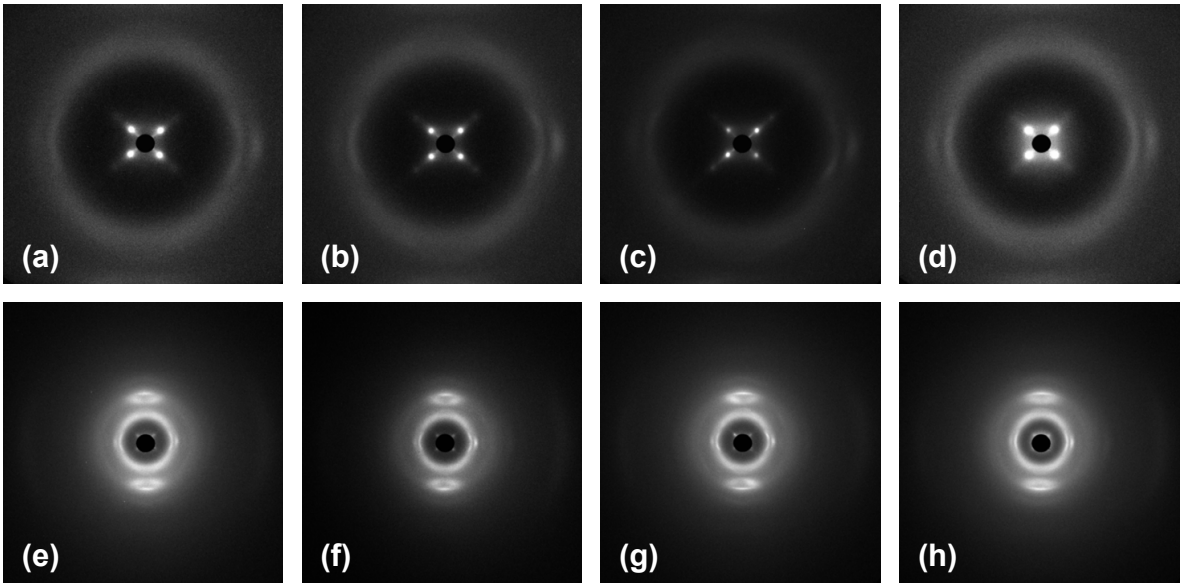

Figure S1. Wide-angle x-ray scattering images of ***5H-5tB*** LCEs that were oriented using a shape memory cycle run using 100 kPa as the maximum applied stress. The stretch direction is horizontal. The top row images (a-d) were collected at a sample to detector distance of 236.4 mm, and the bottom row images (e-h) were collected at a sample to detector distance of 65.7 mm. The patterns are paired by composition and are as follows: **E-*5H*$_{70}$*5tB*$_{30}$** (a, e), **E-*5H*$_{80}$*5tB*$_{20}$** (b, f), **E-*5H*$_{90}$*5tB*$_{10}$** (c, g), and **E-*5H*$_{100}$*5tB*$_{0}$** (d, h).

Differential Scanning Calorimetry. The DSC of **E-*5H*$_{80}$*5tB*$_{20}$** after annealing for one hour at 50 °C shown in Figure S2 is the same trace presented in Figure 2, but here the temperature and heat flow scales are expanded to show T_g more clearly. The dashed lines mark the heat flow signals before and after the transition. The vertical line marks the T_g and is located at the temperature that corresponds to half of the step in the heat flow signal, as described in the Experimental section of this paper.

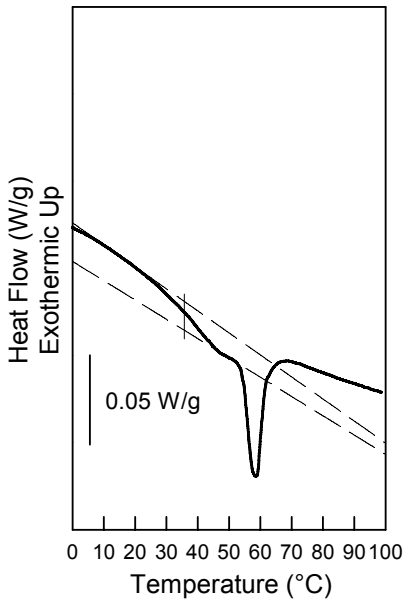

Figure S2. DSC heating trace of **E-*5H*$_{80}$*5tB*$_{20}$** after annealing for one hour at 50 °C. This is the same data shown in Figure 2, but the temperature and heat flow scales have been expanded. Vertical line marks T_g.

Regression analysis of stepped isothermal recovery experiment. To fit strain recovered during the stepped isothermal experiment of **E-*5H*$_{80}$*5tB*$_{20}$** (Fig. 6), each isothermal hold was considered separately and the time where the isothermal commenced was set equal to zero. In all cases, regression lines of the form $\varepsilon = \varepsilon_o + Ae^{-t/\tau}$ fit the data well ($R^2 \geq 0.998$), and the normalized prefactor, A/ε_o, and relaxation time, τ, were determined from these. The stepped isothermal experiment was repeated four times. The normalized prefactors and relaxation times reported in Fig. 7 are the averages from these experiments, and the error bars denote standard deviation. Figure S3 shows a plot of strain versus time for isothermals at 49 °C, 55 °C, and 57 °C. Both the strain for the experimental data (black points) and the regression lines (gray lines) were plotted after first subtracting ε_o.

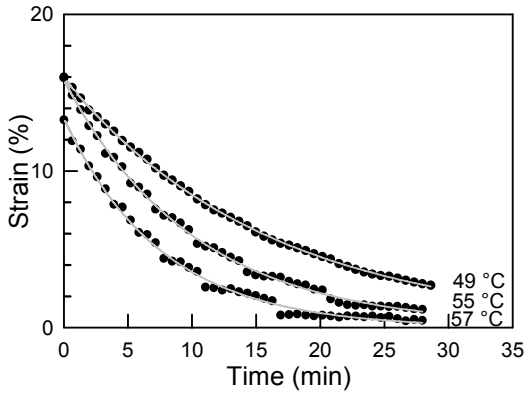

Figure S3. Isothermal recovery of the fixed **E-*5H*$_{80}$*5tB*$_{20}$** at 49 °C, 55 °C, and 57 °C. These isothermals were selected from the full stepped isothermal recovery experiment shown in Fig. 6. Both the experimental data (black circles) and regression fits (gray lines) were normalized by subtracting ε_o from their strain values to give the plot shown.

Supplementary Material (ESI) for Journal of Materials Chemistry

Microstructural changes during shape memory recovery. The plot of relaxation time versus recovery temperature (Figure 7b) showed that the temperature dependence of relaxation time is negligible below the glass transition. Once above the glass transition, relaxation time decreases and the normalized prefactor (Figure 7a) increases with increasing temperature, indicating the devitrification of the mesogens and the release of the network chains for strain recovery. A detailed analysis of microstructural changes during shape memory recovery (subject of future publications) showed similar behavior for mesogen tilt angle. Those experiments studied **E-*5H*$_{80}$*5tB*$_{20}$** as it was recovered from a fixed state at an initial strain of 194 %. The sample was first studied with WAXS, after which it was recovered isothermally at a given temperature before studying again with WAXS. This process was repeated for many temperatures. Patterns collected at a 65.7 mm sample to detector distance and mesogen tilt angle for selected recovery temperatures are shown below. The patterns show that one of the mesogen reflections (boxed on the 25 °C pattern) are initially split. These reflections remain relatively unchanged in their position while the mesogens are in their glassy state, but they do move apart as recovery temperature is increased. Similarly, the mesogen tilt angle decreases only slightly while the mesogens are glassy, however the mesogen tilt angle shows a strong temperature dependence once the mesogens devitrify.

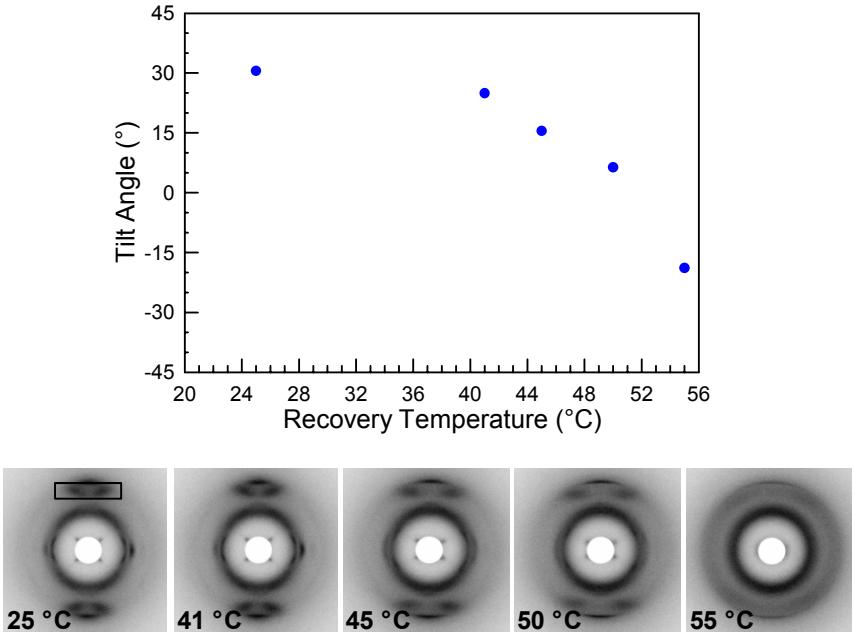

Figure S4. Changes in mesogen tilt angle in **E-*5H*$_{80}$*5tB*$_{20}$** as it is recovered from a fixed state at an initial strain of 194 %. The sample was recovered in a series of isothermal steps, and after each recovery, it was analyzed with WAXS to study its microstructure. Shown are mesogen tilt angle and the WAXS patterns at 65.7 mm for selected recovery temperatures that are noted on the patterns. The box around the mesogen reflections in the 25 °C pattern highlight the reflections that shift during recovery, and the strain axis is horizontal.